LETTER

doi:10.1038/nature11519

Increased HIV-1 vaccine efficacy against viruses with genetic signatures in Env V2

Morgane Rolland[1]*, Paul T. Edlefsen[2]*, Brendan B. Larsen[3], Sodsai Tovanabutra[1], Eric Sanders-Buell[1], Tomer Hertz[2], Allan C. deCamp[2], Chris Carrico[4,5], Sergey Menis[4,5], Craig A. Magaret[2], Hasan Ahmed[2], Michal Juraska[2], Lennie Chen[3], Philip Konopa[3], Snehal Nariya[3], Julia N. Stoddard[3], Kim Wong[3], Hong Zhao[3], Wenjie Deng[3], Brandon S. Maust[3], Meera Bose[1], Shana Howell[1], Adam Bates[1], Michelle Lazzaro[1], Annemarie O'Sullivan[1], Esther Lei[1], Andrea Bradfield[1], Grace Ibitamuno[1], Vatcharain Assawadarachai[6], Robert J. O'Connell[1], Mark S. deSouza[6], Sorachai Nitayaphan[6], Supachai Rerks-Ngarm[7], Merlin L. Robb[1], Jason S. McLellan[8], Ivelin Georgiev[8], Peter D. Kwong[8], Jonathan M. Carlson[9], Nelson L. Michael[1], William R. Schief[4,5], Peter B. Gilbert[2]*, James I. Mullins[3]* & Jerome H. Kim[1]*

The RV144 trial demonstrated 31% vaccine efficacy at preventing human immunodeficiency virus (HIV)-1 infection[1]. Antibodies against the HIV-1 envelope variable loops 1 and 2 (Env V1 and V2) correlated inversely with infection risk[2]. We proposed that vaccine-induced immune responses against V1/V2 would have a selective effect against, or sieve, HIV-1 breakthrough viruses. A total of 936 HIV-1 genome sequences from 44 vaccine and 66 placebo recipients were examined. We show that vaccine-induced immune responses were associated with two signatures in V2 at amino acid positions 169 and 181. Vaccine efficacy against viruses matching the vaccine at position 169 was 48% (confidence interval 18% to 66%; $P = 0.0036$), whereas vaccine efficacy against viruses mismatching the vaccine at position 181 was 78% (confidence interval 35% to 93%; $P = 0.0028$). Residue 169 is in a cationic glycosylated region recognized by broadly neutralizing and RV144-derived antibodies. The predicted distance between the two signature sites (21 ± 7 Å) and their match/mismatch dichotomy indicate that multiple factors may be involved in the protection observed in RV144. Genetic signatures of RV144 vaccination in V2 complement the finding of an association between high V1/V2-binding antibodies and reduced risk of HIV-1 acquisition, and provide evidence that vaccine-induced V2 responses plausibly had a role in the partial protection conferred by the RV144 regimen.

Vaccination with the RV144 regimen (ALVAC-HIV and AIDSVAX B/E gp120) afforded an estimated 31% protection against HIV-1 acquisition[1]. Two immune correlates of infection risk were identified: plasma IgA antibodies to Env were associated with increased risk, and IgG binding to Env V1/V2 with decreased risk[2]. These analyses compared HIV-1-infected and uninfected vaccine recipients and established correlates of risk[3,4], which are not necessarily predictive of protection as immune responses are not randomized among vaccinees. In contrast, sieve analyses[5–7] compare breakthrough viruses in vaccine and placebo recipients, leveraging the randomization to causally attribute observed differences between HIV-1 sequences to the vaccine. Sieve analyses look for evidence that vaccine-induced immune responses selectively block certain viruses and/or drive escape mutations post-infection, and interrogate treatment differences in HIV-1 sequences derived at the time of HIV-1 diagnosis as evidence for this effect.

We proposed that RV144 vaccine-induced antibodies to Env V1/V2 could selectively prevent HIV-1 infections by certain variants, and that this effect would be evident in the V1/V2 region of breakthrough viruses. To test this hypothesis, we examined the relationship between vaccine status and V1/V2 sequence characteristics using 936 HIV-1 sequences from 110 breakthrough infections: 44 vaccine and 66 placebo recipients (focusing on subjects infected with HIV-1 CRF01_AE, that is, 110 of the 121 characterized infections that occurred after the first immunization). One epidemiologically known transmission pair was confirmed by phylogenetic reconstructions; thus, sensitivity analyses were performed after removing sequences from the individual who was the second to become HIV-1 infected to preserve independence of infection events.

Our analysis focused on HIV-1 sequences corresponding to the glycoprotein 70 gp70-V1/V2 clade B reagent used to identify the correlate of risk (amino acids 120 to 204 of the reference sequence HXB2). Supplementary Methods 1 summarize the pre-filtering of sites that was performed as pre-specified to increase statistical power. First, sites that were invariant or where there was little confidence in the alignment were excluded. Then, sites were selected following two approaches. The first approach, termed 'contact residues', required that sites were both (1) known contact residues for monoclonal antibodies or had been implicated as such in neutralization sensitivity assays[8–11], and (2) 'hotspots' of vaccine-induced binding antibody reactivity from a linear peptide binding microarray analysis of uninfected RV144 vaccine recipients. The 'contact residues' approach yielded eight sites for analysis: HXB2 positions 120, 124, 165, 166, 168, 169, 171 and 181. The second approach, called EPIMAP (epitope prediction by interrogating conformational ensembles of glycosylated antigens with a multi-oriented antibody probe), was based on structural predictions of antibody epitopes: thousands of potential antibody epitopes (centred on gp120 surface residues for the three Env in the vaccine) were predicted and used to rank V1/V2 sites by their likelihood of being antibody targets. The EPIMAP approach yielded 12 high-ranking sites: HXB2 positions 160, 166, 168–173, 178, 179, 181 and 197.

To test if vaccination (through vaccine-induced antibodies to Env V1/V2) protected against acquisition of certain HIV-1 variants, we adapted the primary analysis method used previously[1] to assess vaccine efficacy against HIV-1 genotypes differing at the 15 selected sites identified by either the 'contact residues' or EPIMAP approaches (Supplementary Table 1 and Supplementary Fig. 2; note that vaccine efficacy is estimated based on all RV144 participants, that is, 8,197 vaccine and 8,198 placebo recipients). We found that vaccine efficacy significantly differed for HIV-1 genotypes defined by whether they presented a residue matching the vaccine insert (or not) at position

[1]US Military HIV Research Program, Silver Spring, Maryland 20910, USA. [2]Statistical Center for HIV/AIDS Research and Prevention, Vaccine and Infectious Disease Division, Fred Hutchinson Cancer Research Center, Seattle, Washington 98109, USA. [3]Department of Microbiology, University of Washington, Seattle, Washington 98195, USA. [4]Department of Biochemistry, University of Washington, Seattle, Washington 98195, USA. [5]IAVI Neutralizing Antibody Center and Department of Immunology and Microbial Sciences, The Scripps Research Institute, La Jolla, California 92037, USA. [6]Royal Thai Army Component, AFRIMS, Bangkok 10400, Thailand. [7]Thai Ministry of Public Health, Nonthaburi 11000, Thailand. [8]Vaccine Research Center, NIAID, NIH, Bethesda, Maryland 20892, USA. [9]Microsoft Research, Redmond, Washington 98052, USA.

*These authors contributed equally to this work.

169 ($P = 0.034$) and 181 ($P = 0.024$) (Table 1). The estimated cumulative HIV-1 incidence curves in the vaccine and placebo groups illustrate vaccine efficacy for two genotypes (K169 and I181X) and no efficacy for the opposite residues (Supplementary Fig. 2) (diagnostic tests did not show significant evidence of violation of the proportional hazards assumption), and the cumulative HIV-1 incidence curves showed a trend towards waning vaccine effect on genotype over time, analogous to the temporal effect on efficacy seen in RV144[1,12]. The estimated vaccine efficacy against viruses matching the vaccine at position 169 (K169) was 48% ($P = 0.0036$; 95% confidence interval (CI): 18%, 66%), whereas vaccine efficacy versus position-169-mismatched viruses was not significant. Vaccine efficacy against viruses differing from the vaccine insert at 181 (181X) was 78% ($P = 0.0028$; 95% CI: 35%, 93%), whereas vaccine efficacy versus vaccine-matched viruses at that site was not significant. Furthermore, vaccine efficacy against viruses that were both 169-matched and 181-mismatched was 80% ($P = 0.0046$; CI: 31%, 94%). These results indicate that vaccine-induced immune responses to the Env V2 may have blocked infections with viruses matching the vaccine at K169 and differing from the vaccine at I181. We applied the statistical method from ref. 2 to test whether gp70-V1/V2 antibodies and V2 'hotspot' antibodies were correlates of risk of infection for specific HIV-1 genotypes. The estimated association of these antibodies with genotype-specific infection risk was similar across the genotypes, such that the sieve effects are not explained by these antibody correlates. However, there is low power to detect differences by genotype because only 34 infected vaccinees could be included in the analysis (see Supplementary Table 2).

To further evaluate site-specific differences between viruses from vaccine and placebo recipients, we applied three additional site-scanning methods to both the 'contact residues' and 'EPIMAP' sets of sites: the nonparametric weighted distance comparison test (GWJ)[13], the mismatch bootstrap method (MMBootstrap)[7], and a model-based method that is more sensitive to differences in non-insert amino acid frequencies[14]. Based on both the 'contact residues' and 'EPIMAP'-derived sets of sites, the most general method GWJ identified positions 169 and 181 as significantly distinguishing HIV-1 sequences from vaccine and placebo recipients (Figs 1 and 2). These two sites showed significant or borderline significant results with the additional site-scanning methods (MMBootstrap and model-based) (Supplementary Table 3). These results were corroborated after excluding a subject from the transmission pair: results were consistent although with weaker statistical support. As pre-specified, corrections for multiple testing were performed separately for each analysis method and for each of the three vaccine insert sequences; no correction for multiple tests was applied across the tests because these are considered sensitivity analyses meant to evaluate congruence.

The fact that our sequence data were obtained through an effectively implemented randomized trial[15] reduces the need for phylogenetic corrections as performed in observational studies (Supplementary Note 1). Nonetheless, to potentially assess mechanisms behind sieve effects, we tested the impact of shared ancestry among viruses in our data set with phylogenetic dependency networks[16] and independent contrasts[17]. Both approaches found that the sieve effect at site 181 was independent of the tree topology, whereas that of site 169 was not (Supplementary Tables 4 and 5); these results must be interpreted with caution because the sequence data were used both to infer the phylogenetic tree and to evaluate sieve effects[17].

In agreement with the vaccine efficacy results, the consensus amino acid K169 was more frequently different from the CRF01_AE vaccine sequence among viruses from vaccinees, whereas site 181, the third position of the putative tri-peptide $\alpha_4\beta_7$ integrin binding motif, was more likely to be similar to the vaccine sequence in vaccinees. When we tested whether sites in the two groups were evolving under different selective pressures along internal tree branches, likelihood ratio test results[18] provided evidence that site 169 was under differential pressure across treatment arms ($P = 0.043$ based on data set with 110 subjects; $P = 0.064$ based on 109 subjects) (Supplementary Table 6).

HIV-1 variants with K169X might have had longer V2 loops (mean = 43.2 (interquartile range (IQR): 40–46) versus 41.9 (IQR: 39–44), $P = 0.11$) and more potential N-linked glycosylation sites (PNGS) (mean = 2.44 (IQR: 2–3) versus 2.12 (IQR: 2–3), $P = 0.08$) than K169 viruses (Supplementary Table 7). Although the latter P values were not significant, longer loops and increased PNGS have been associated with reduced sensitivity to neutralization[19]. The trend towards longer V2 and more PNGS in individuals with K169X was apparently not explained by a longer duration of HIV-1 infection (no difference in the time since the last HIV-1-negative visit used as a proxy for the duration of HIV-1 infection (K169X versus K169: median = 181 versus 179, mean = 250 versus 207, $P = 0.41$)) (Supplementary Table 7). Furthermore, studies with quaternary-structure-preferring (QSP) antibodies (for example, PG9, PG16, CH01-04 and PGT141-145) showed that mutations at positions 169 and 181 were associated with significant alterations in neutralization[10,20]. Some strains became sensitive to QSP antibodies by mutating residue 169 to K[21]. These results indicate that K169X mutations could be a mechanism for avoidance of QSP antibodies and potentially other V2-specific antibodies. Indeed, the epitope of CH58, an anti-V2 monoclonal antibody isolated from an RV144 vaccine recipient, spanned amino acids 167–180 and position 169 was critical for binding (Liao, H.-X. *et al.*, personal communication).

To explore whether the sieve effects at sites 169 and 181 were linked, we looked at structural data and covariability. We found no conclusive evidence suggesting that the two sites were contained within the same epitope. The Cα–Cα distance between residues 169 and 181 was 21 ± 7 Å (mean ± s.d.) on the basis of the 3,000 low-energy all-atom models computed for the three vaccine inserts (Supplementary Table 8), whereas sites 169 and 181 were more than 30 Å apart in the crystal structure of J08-scaffolded HIV-1 gp120 V1/V2 bound to the broadly neutralizing monoclonal antibody PG9 (ref. 22; Supplementary Fig. 3). The two sites could lie in a single antibody epitope because the average diameter of antibody-bound epitopes was predicted to be 30.5 Å (on

Table 1 | Estimated vaccine efficacies to prevent infection with specific HIV-1 genotypes, and estimated ratios of hazard ratios

Genotype	Number of infections		Vaccine efficacy (95% CI)	*P* value
	Vaccine	Placebo		
Overall	44	66	34% (7.8%, 54.7%)	0.034
K169	**30**	**57**	**48% (18%, 66%)**	**0.0036**
K169X	14	9	−55% (−258%, 33%)	0.3
I181	40	48	17% (−26%, 45%)	0.38
I181X	**4**	**18**	**78% (35%, 93%)**	**0.0028**
K169-I181	27	42	36% (−4%, 61%)	0.071
K169-I181X	**3**	**15**	**80% (31%, 94%)**	**0.0046**
K169X-I181	13	6	−116% (−467%, 19%)	0.11
K169X-I181X	1	3	67% (−219%, 97%)	0.32
			Estimated HR/HR* (95% CI)	***P* value**
K169X/K169			**2.73 (1.08, 6.92)**	**0.034**
I181/I181X			**3.77 (1.19, 11.92)**	**0.024**
Else/K169-I181			1.04 (0.49, 2.22)	0.92
Else/K169-I181X			1.85 (0.79, 4.32)	0.16
K169X-I181/Else			**2.76 (1.23, 6.20)**	**0.014**
Else/K169X-I181X			1.06 (0.40, 2.86)	0.9

Shown are estimated vaccine efficacies (vaccine efficacies = 1 − hazard ratios (HRs)) to prevent infection with specific HIV-1 genotypes, and estimated ratios of HRs measuring the relative protection against given pairs of HIV-1 genotypes.

* Each HR is the hazard ratio (vaccine versus placebo) of HIV-1 infections with a particular genotype. For example, for the K169X/K169 entry, the numerator HR measures the vaccine effect to prevent HIV-1 infections with K169X-variants and the denominator HR measures the vaccine effect to prevent HIV-1 infections with K169-variants, and the result 2.73 means that the vaccine lowers the rate of infection 2.73-times more against K169-matched HIV-1 viruses than against K169-mismatched HIV-1 infections, that is, the level of protection is 2.73 greater against K169-matched than against K169-mismatched HIV-1 viruses (that is against all viruses with a residue differing from K at site 169).
Else: all genotypes other than the joint genotype under consideration.

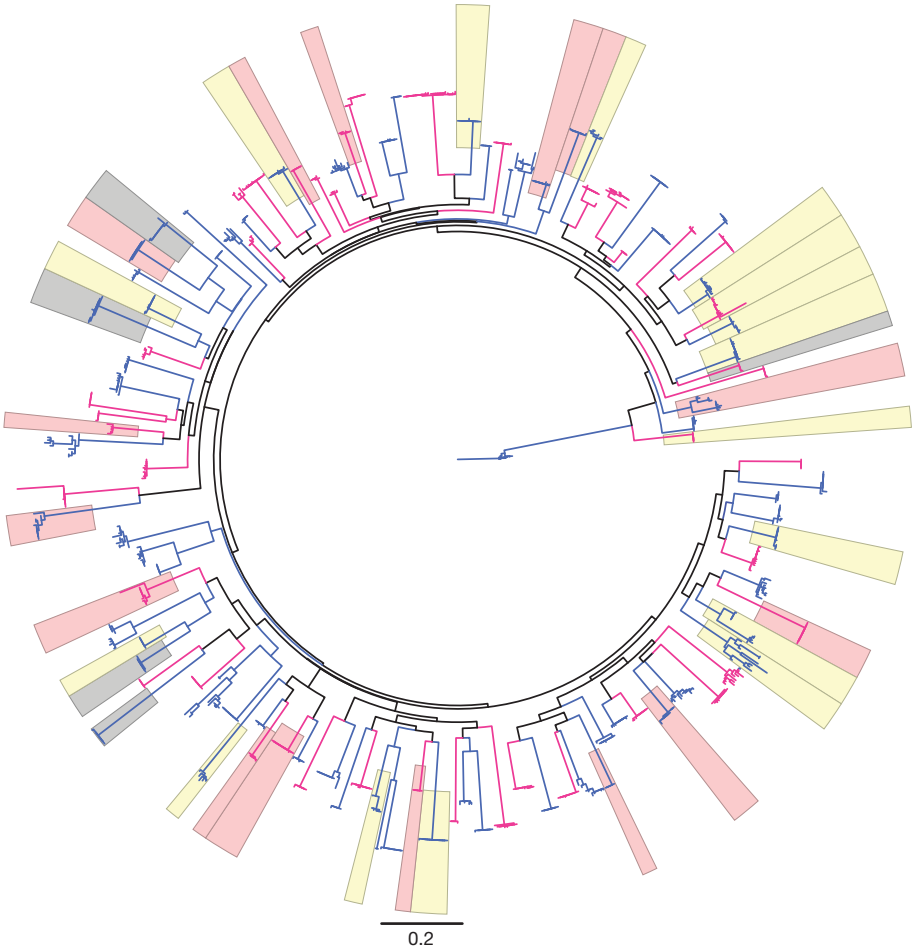

Figure 1 | Phylogenetic tree of *env-V1/V2* nucleotide sequences. Highlights are used for sequences presenting mutations at either site 169 (in pink) or 181 (in yellow) or at both sites (in grey). Sequences from vaccine recipients are figured in red, those from placebo recipients are in blue.

the basis of 32 pairs of bound antigen structures[23]). Furthermore, we found no evidence that the sieve effect at site 181 was linked to site 169 by analysing covariation on pre-selected V1/V2 sites[24,25]. We noted covariability in the mid-V2 loop, which corresponds to the binding site of the V1/V2-specific mAb from RV144 (ref. 2 and personal communication, Liao H.-X. *et al.*, Supplementary Table 9).

The unexpected sieve effect at site 181 showing greater vaccine efficacy against mismatched HIV-1 indicates a vaccine-induced constraint that either hindered the establishment of infection with I181X variants or promoted infections with I181 variants. Although it is plausible that vaccine-induced antibodies enhanced HIV-1 infections with I181 variants, there was no statistical support for such enhancement because there was no evidence of negative vaccine efficacy against I181 viruses: estimated vaccine efficacy = 17%, 95% CI = −26% to 45%, $P = 0.38$ (Table 1). Other hypotheses include: (1) the stricter conservation at site 181 may be a marker of a non-identified sequence characteristic (possibly linked to the variable loop that starts a few amino acids downstream of 181), (2) specific variants may be unable to establish infection due to steric/quaternary structure constraints with vaccine-induced antibodies, and (3) I181X viruses may be preferentially targeted by vaccine-induced antibodies.

Sieve analysis is an important component of assessing immune correlates of protection because it compares vaccine to placebo recipients and could identify selective pressures below the level of detection of standard immune assays[7]. Our V1/V2-focused analysis leveraged randomized treatment assignments to establish a causal connection between vaccination and a selective filtering of V1/V2 variants. The identification of signatures in V2 provides a corroborative

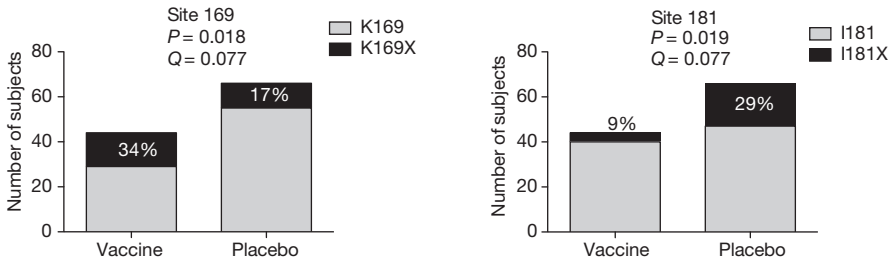

Figure 2 | Bar graphs representing the mutations at positions 169 and 181 based on sequences from 44 vaccine and 66 placebo recipients. The *P* and *Q* values correspond to the site-scanning sieve analysis method GWJ. The values correspond to comparisons against the 92TH023 vaccine insert based on the selected sites identified through the 'contact residues' approach. Pre-specified *P* value and *Q* value significance thresholds of 0.05 and 0.2, respectively. Full results in Supplementary Table 3.

virological determinant to the V1/V2 antibodies correlate of risk[2] and highlights the mid-V2 loop as an important target for antibody-mediated prevention of HIV-1 infection, but also suggests that vaccine efficacy is ablated by viral sequences with signature sequence variants, raising the possibility of population-level adaptation to the vaccine. Given the 31% efficacy against infection afforded by the vaccine and the suspected mechanism of action of V1/V2 antibody, our analysis suggests that specific HIV-1 variants were blocked from establishing HIV-1 infection (an acquisition sieve effect); however, viral sequences may also have mutated in response to vaccine-induced immune pressure, corresponding to a post-infection sieve effect. Further studies with infectious molecular clones carrying V1/V2 signature mutations are needed to clarify their role in viral infectivity, fitness and escape. Together, these results vouch for sieve analysis as an integral part of the search for immune correlates of protection in vaccine studies and show that sieve analysis can be a powerful tool to assess the efficacy of new vaccine candidates.

METHODS SUMMARY

Viral genomes were amplified by endpoint-dilution PCR of viral RNA from plasma specimens collected at the time of HIV-1 diagnosis, and were directly sequenced[7]. Sites in Env V/1V2 were selected for statistical testing using two approaches: one based on a peptide binding microarray assay, known antibody contact sites and literature, the other based on a computational prediction algorithm of antibody binding sites. Each site was tested with four site-scanning sieve analysis methods to identify those that discriminated the vaccine and placebo group. Genotype-specific vaccine efficacy was assessed with the Cox proportional hazards model and score test as described previously[25], and differential vaccine efficacy by genotype was assessed with the model described in refs 26,27. Three additional methods were designed to compare the subjects' sequences to the vaccine insert sequences (a subtype B (MN) and two CRF01_AE strains, 92TH023 and CM244): a nonparametric weighted distance comparison test (GWJ)[12], a mismatch bootstrap method (MMBootstrap)[7] and a model-based Bayesian-frequentist hybrid method that is more sensitive to differences in non-insert amino acid frequencies[13]. The GWJ method computes a two-sample pooled-variance *t*-statistic and compares this statistic to a permutation-derived null distribution. The MMBootstrap method computes the difference in the fraction of mismatches to the insert amino acids using all available sequences, and compares this to a bootstrap-derived null distribution. The model-based method compares the posterior probability of a sieve effect to a null distribution for a Bayesian multinomial model. A *Q*-value multiplicity adjustment procedure was pre-specified to limit the false discovery rate to 20% (ref. 28). Covariation was detected using the Kullback–Leibler divergence and differential tests[23], and a Bayesian graphical method[24]. A schematic description of the study is found in Supplementary Fig. 1.

Full Methods and any associated references are available in the online version of the paper.

Received 25 April; accepted 24 August 2012.
Published online 10 September 2012.

1. Rerks-Ngarm, S. *et al.* Vaccination with ALVAC and AIDSVAX to prevent HIV-1 infection in Thailand. *N. Engl. J. Med.* **361,** 2209–2220 (2009).
2. Haynes, B. F. *et al.* Immune-correlates analysis of an HIV-1 vaccine efficacy trial. *N. Engl. J. Med.* **366,** 1275–1286 (2012).
3. Plotkin, S. A. & Gilbert, P. B. Nomenclature for immune correlates of protection after vaccination. *Clin. Infect. Dis.* **54,** 1615–1617 (2012).
4. Rolland, M. & Gilbert, P. Evaluating immune correlates in HIV type 1 vaccine efficacy trials: what RV144 may provide. *AIDS Res. Hum. Retroviruses* **28,** 400–404 (2012).
5. Gilbert, P. B., Self, S. G. & Ashby, M. A. Statistical methods for assessing differential vaccine protection against human immunodeficiency virus types. *Biometrics* **54,** 799–814 (1998).
6. Gilbert, P., Self, S., Rao, M., Naficy, A. & Clemens, J. Sieve analysis: methods for assessing from vaccine trial data how vaccine efficacy varies with genotypic and phenotypic pathogen variation. *J. Clin. Epidemiol.* **54,** 68–85 (2001).
7. Rolland, M. *et al.* Genetic impact of vaccination on breakthrough HIV-1 sequences from the STEP trial. *Nature Med.* **17,** 366–371 (2011).
8. Wei, X. *et al.* Antibody neutralization and escape by HIV-1. *Nature* **422,** 307–312 (2003).
9. Moore, P. L. *et al.* Limited neutralizing antibody specificities drive neutralization escape in early HIV-1 subtype C infection. *PLoS Pathog.* **5,** e1000598 (2009).
10. Tomaras, G. D. *et al.* Polyclonal B cell responses to conserved neutralization epitopes in a subset of HIV-1-infected individuals. *J. Virol.* **85,** 11502–11519 (2011).
11. Lynch, R. M. *et al.* The B cell response is redundant and highly focused on V1V2 during early subtype C infection in a Zambian seroconverter. *J. Virol.* **85,** 905–915 (2011).
12. Robb, M. L. *et al.* Risk behaviour and time as covariates for efficacy of the HIV vaccine regimen ALVAC-HIV (vCP1521) and AIDSVAX B/E: a post-hoc analysis of the Thai phase 3 efficacy trial RV 144. *Lancet Infect. Dis.* **12,** 531–537 (2012).
13. Gilbert, P. B., Wu, C. & Jobes, D. V. Genome scanning tests for comparing amino acid sequences between groups. *Biometrics* **64,** 198–207 (2008).
14. Edlefsen, P. T. Model-based sieve analysis. Preprint at http://arxiv.org/abs/1206.6701 (2012).
15. Gilbert, P. B. *et al.* Statistical interpretation of the RV144 HIV vaccine efficacy trial in Thailand: a case study for statistical issues in efficacy trials. *J. Infect. Dis.* **203,** 969–975 (2011).
16. Carlson, J. M. *et al.* Phylogenetic dependency networks: inferring patterns of CTL escape and codon covariation in HIV-1 Gag. *PLoS Comput. Biol.* **4,** e1000225 (2008).
17. Felsenstein, J. Phylogenies and the comparative method. *Am. Nat.* **125,** 1–15 (1985).
18. Pond, S. L. & Frost, S. D. Datamonkey: rapid detection of selective pressure on individual sites of codon alignments. *Bioinformatics* **21,** 2531–2533 (2005).
19. Derdeyn, C. A. *et al.* Envelope-constrained neutralization-sensitive HIV-1 after heterosexual transmission. *Science* **303,** 2019–2022 (2004).
20. Moore, P. L. *et al.* Potent and broad neutralization of HIV-1 subtype C by plasma antibodies targeting a quaternary epitope including residues in the V2 loop. *J. Virol.* **85,** 3128–3141 (2011).
21. Doria-Rose, N. A. *et al.* A short segment of the HIV-1 gp120 V1/V2 region is a major determinant of resistance to V1/V2 neutralizing antibodies. *J. Virol.* **86,** 8319–8323 (2012).
22. McLellan, J. S. *et al.* Structure of HIV-1 gp120 V1/V2 domain with broadly neutralizing antibody PG9. *Nature* **480,** 336–343 (2011).
23. Rubinstein, N. D. *et al.* Computational characterization of B-cell epitopes. *Mol. Immunol.* **45,** 3477–3489 (2008).
24. Gilbert, P. B., Novitsky, V. & Essex, M. Covariability of selected amino acid positions for HIV type 1 subtypes C and B. *AIDS Res. Hum. Retroviruses* **21,** 1016–1030 (2005).
25. Poon, A. F., Lewis, F. I., Pond, S. L. & Frost, S. D. An evolutionary-network model reveals stratified interactions in the V3 loop of the HIV-1 envelope. *PLoS Comput. Biol.* **3,** e231 (2007).
26. Prentice, R. L. *et al.* The analysis of failure times in the presence of competing risks. *Biometrics* **34,** 541–554 (1978).
27. Lunn, M. & McNeil, D. Applying Cox regression to competing risks. *Biometrics* **51,** 524–532 (1995).
28. Grambsch, P. & Therneau, T. M. Proportional hazards tests and diagnostics based on weighted residuals. *Biometrika* **81,** 515–526 (1994).

Supplementary Information is available in the online version of the paper.

Acknowledgements We thank B. F. Haynes and F. A. Matsen for advice and comments, and I. A. Wilson and R. L. Stanfield for assistance. This study was supported in part by an Interagency Agreement Y1-AI-2642-12 between US Army Medical Research and Material Command (USAMRMC) and the National Institutes of Allergy and Infectious Diseases. This work was also supported by a cooperative agreement (W81XWH-07-2-0067) between the Henry M. Jackson Foundation for the Advancement of Military Medicine, Inc., and the US Department of Defense (DOD). Additional support was provided to P.B.G. through the NIH grant 2R37AI05465-10. The opinions herein are those of the authors and should not be construed as official or representing the views of the US Department of Defense or the Department of the Army.

Author Contributions M.R. conducted the sequence analysis with contributions from B.B.L., W.D. and B.S.M.; P.T.E. and P.B.G. conducted the site-scanning sieve analyses. M.R., S.T., E.S.-B. and J.I.M. designed the sequencing experiments. B.B.L., L.C., P.K., S.N., J.N.S., K.W., H.Z., M.B., S.H., A. Bates, M.L., A.O'S., E.L., A. Bradfield, G.I. and V.A. performed viral sequencing. T.H., A.C.deC., C.A.M., H.A. and M.J. contributed statistical analyses. C.C., S.M. and W.R.S. developed the EPIMAP approach. J.S.M., I.G. and P.D.K. identified antibody contact residues and performed V2 structural analyses. J.M.C. performed phylogenetic dependency network analyses. R.J.O'C., M.S.deS., S.N., S.R.-N., M.L.R., N.L.M. and J.H.K. conducted the RV144 trial. M.R., P.T.E., P.B.G., J.I.M. and J.H.K. designed the studies, analysed data, prepared the manuscript (with contributions from J.M.C., P.D.K. and W.R.S.) and supervised the project.

Author Information Sequences are available under GenBank accession numbers JX446645–JX448316. Reprints and permissions information is available at www.nature.com/reprints. The authors declare no competing financial interests. Readers are welcome to comment on the online version of the paper. Correspondence and requests for materials should be addressed to M.R. (mrolland@hivresearch.org).

METHODS

Study design. The protocol was approved by the Institutional Review Boards of the Ministry of Public Health, the Royal Thai Army, Mahidol University, and the US Army Medical Research and Materiel Command. Written informed consent was obtained from all participants. The vaccine regimen consisted of four injections (at 0, 1, 3 and 6 months) of ALVAC-HIV[vCP1521], which expresses gp120 of CRF01_AE (92TH023), and two injections (at 3 and 6 months) with AIDSVAX B/E which is composed of two gp120 proteins truncated at the amino terminus (start at amino acid 42): MN (subtype B) and CM244 (CRF01_AE).

HIV-1 sequencing. Viral genomes were amplified by endpoint-dilution PCR of viral RNA from plasma specimens collected at the time of HIV-1 diagnosis, and were directly sequenced based on methods adapted from ref. 7. Briefly, a first round near-full-length genome polymerase chain reaction (PCR) was done with the Advantage LA Polymerase (50-μl reaction), followed by a real-time PCR (TaqMan Gene Expression Master Mix) on 5 μl of the first round product for the detection of HIV-1 *gag* (186 bp) and *env* (232 bp). For first-round products identified as endpoint-positive by real-time PCR, 2 μl were subjected to a second-round amplification using KAPA LR HS DNA polymerase. A re-amplification using 1 μl of the first-round product (dilution factor: 1 to 100) with second-round PCR primers is performed to obtain sufficient material for sequencing. PCR and sequencing primers are listed in Supplementary Tables 10 and 11.

EPIMAP. Potential patches, defined by lists of residues and atoms within each putative antibody epitope, were predicted for each vaccine insert using an unbiased, exhaustive, structure-based computational approach taking into account vaccine-specific orientational constraints. Full-length glycosylated vaccine inserts were threaded onto known structures of gp120 and regions not crystallized were built *de novo*. Each model was interrogated by a full-atom antibody probe placed at multiple rotations and orientation vectors were centred on each amino acid. The proportion of patches containing a given V1/V2 site were calculated for each insert (Supplementary Fig. 4) and the top-ranking V1/V2 sites were selected based on the average of the percentages for the prime (92TH023) and the max of the two boost proteins (MN,CM244), yielding 22 sites (Supplementary Fig. 5) of which 12 passed the conservation and alignability criteria (described in Supplementary Table 1).

Filtering of V1/V2 sites. Procedure described in Supplementary Methods 1.

Vaccine efficacy. Genotype-specific vaccine efficacy was assessed with the Cox proportional hazards model and score test as described previously[26], and differential vaccine efficacy by genotype was assessed with the same model as described previously[27,29]. Vaccine efficacies were calculated based on one representative sequence per individual (the 'mindist': smallest Hamming distance to the subject's consensus sequence) but using all the RV144 participants, including uninfected ones. To test if the proportional hazards assumption was violated for any of the HIV-1 genotypes, we used the Grambsch and Therneau proportional hazards test (based on Schoenfeld residuals)[28].

Sieve analyses. Site-scanning sieve analysis methods evaluate each site to identify those that discriminate the vaccine and placebo group. In addition to the differential vaccine efficacy analysis, the pre-selected sites were tested against the three vaccine insert sequences using three other methods: a nonparametric weighted distance comparison test (GWJ)[13], a mismatch bootstrap method (MMBootstrap) adapted from[7], and a model-based Bayesian-frequentist hybrid method that is more sensitive to differences in non-insert amino acid frequencies[14]. The GWJ method computes a two-sample pooled-variance *t*-statistic and compares this statistic to a permutation-derived null distribution. Each subject contributes a weight that is computed as the from insert amino acid to subject amino acid entry in a (probability-form) substitution matrix using the subject's 'mindist' sequence. The MMBootstrap method computes the difference in the fraction of mismatches to the insert amino acid using all available sequences, and compares this to a bootstrap-derived null distribution (resampling subject labels, not individual sequence labels). The model-based method compares the posterior probability of a sieve effect to a null distribution (estimated by permutation) for a Bayesian multinomial model. All of these methods were verified for control of type-I error rate. A *Q* value multiplicity adjustment procedure was pre-specified to limit the false discovery rate to 20%[30]; it was conducted on a per analysis basis, that is, per insert and per method. Code provided in Supplementary Information 2.

Positive selection. We tested whether the relative rates of synonymous and non-synonymous substitutions in the two groups were significantly different by applying a likelihood ratio test as implemented in Hyphy[18] (http://www.hyphy.org).

Independent contrasts. We used independent contrasts[17] to test if the character state at each tip of the tree was correlated with the length of the branch leading to it, with the assumption of evolution via Brownian motion (that is, neutral evolution). Phylogenetically independent contrasts between the vaccine status and the tip data were calculated in Mesquite (http://mesquiteproject.org/pdap_mesquite/). After the poor fit of the tree to the tip data was verified, contrasts were generated by subtracting one degree of freedom for each polytomy in the tree ($n = 1$) using vaccine status as the dependent variable ('positivized' contrast).

Phylogenetic dependency networks. We used phylogenetic dependency networks to identify associations between the vaccine status and every amino acid position and state, while taking into account the shared ancestry in the HIV-1 phylogeny[16]. A maximum likelihood phylogenetic tree was constructed and a model of conditional adaptation was created for the vaccine status and for every position and state. The null hypothesis is that observations depend on the tree structure; then, adaptation due to each variable is modelled along the tree by an additive process. All results were adjusted for multiple comparisons, using a *Q* value threshold of ≤ 0.2 (implying a false-positive proportion of 20% among identified associations).

Covariation. Associations between residues were detected using the Kullback–Leibler divergence covariation and differential covariation tests[24], and a Bayesian graphical method, which explicitly models the evolutionary history of the sequences[25].

29. Gilbert, P. B. Comparison of competing risks failure time methods and time-independent methods for assessing strain variations in vaccine protection. *Stat. Med.* **19,** 3065–3086 (2000).
30. Storey, J. D. The positive false discovery rate: a Bayesian interpretation and the *q*-value. *Ann. Stat.* **31,** 2013–2035 (2003).